**Supporting Information**

# Targeting the SARS-CoV-2 RNA Dependent RNA Polymerase (RdRp) With Synthetic/Designer Unnatural Nucleoside Analogues: An *In Silico* Study

Subhendu Sekhar Bag*[,a,b], Sayantan Sinha[b], Soumya Dutta[a], Hirak Jyoti Baishya[a] and Suravi Paul[a]

[a]Chemical Biology/Genomics Laboratory, Department of Chemistry, and [b]Centre for the Environment, Indian Institute of Technology Guwahati, India-781039.

* Corresponding Author: Prof. Subhendu Sekhar Bag, CChem, FRSC, FICS; Email: ssbag75@iitg.ac.in

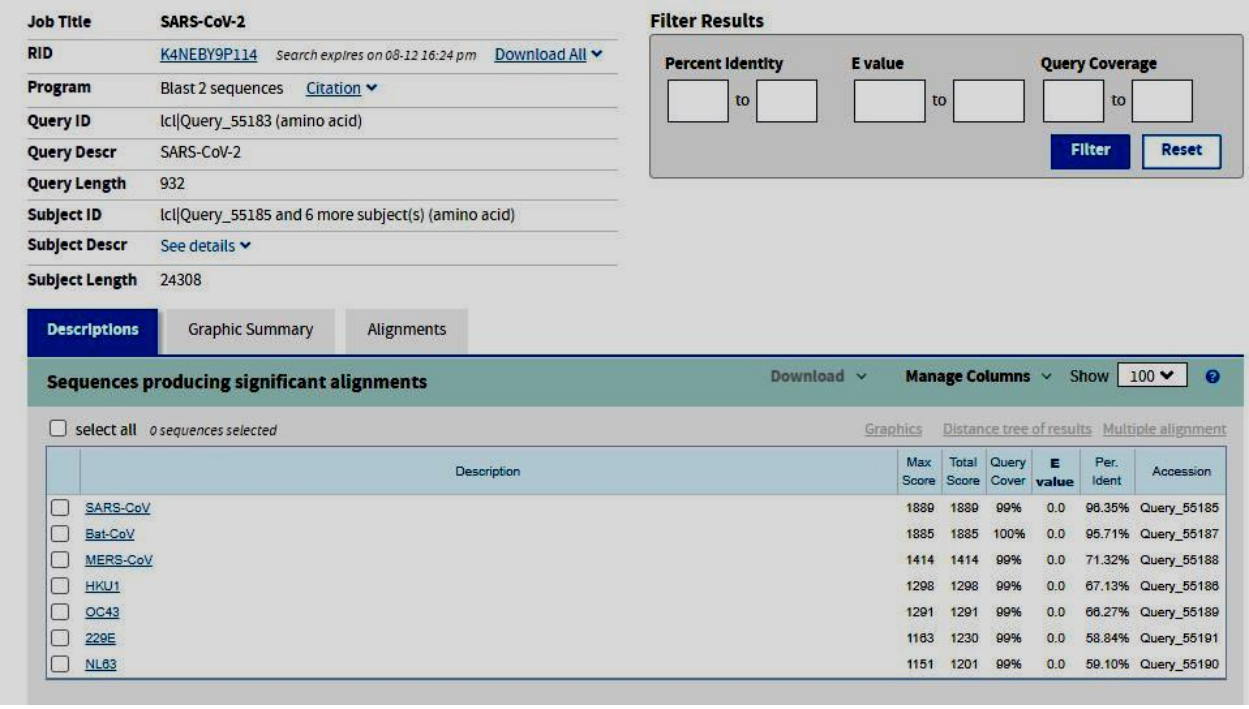

| | |
|---|---|
| Job Title | SARS-CoV-2 |
| RID | K4NEBY9P114 *Search expires on 08-12 16:24 pm* Download All |
| Program | Blast 2 sequences Citation |
| Query ID | lcl\|Query_55183 (amino acid) |
| Query Descr | SARS-CoV-2 |
| Query Length | 932 |
| Subject ID | lcl\|Query_55185 and 6 more subject(s) (amino acid) |
| Subject Descr | See details |
| Subject Length | 24308 |

Filter Results

Percent Identity to | E value to | Query Coverage to | Filter | Reset

Descriptions | Graphic Summary | Alignments

**Sequences producing significant alignments** Download Manage Columns Show 100

select all *0 sequences selected* Graphics Distance tree of results Multiple alignment

| Description | Max Score | Total Score | Query Cover | E value | Per. Ident | Accession |
|---|---|---|---|---|---|---|
| SARS-CoV | 1889 | 1889 | 99% | 0.0 | 96.35% | Query_55185 |
| Bat-CoV | 1885 | 1885 | 100% | 0.0 | 95.71% | Query_55187 |
| MERS-CoV | 1414 | 1414 | 99% | 0.0 | 71.32% | Query_55188 |
| HKU1 | 1298 | 1298 | 99% | 0.0 | 67.13% | Query_55186 |
| OC43 | 1291 | 1291 | 99% | 0.0 | 66.27% | Query_55189 |
| 229E | 1163 | 1230 | 99% | 0.0 | 58.84% | Query_55191 |
| NL63 | 1151 | 1201 | 99% | 0.0 | 59.10% | Query_55190 |

**Figure S1 (a). Percentage identity matrix as obtained from BLASTp study.**

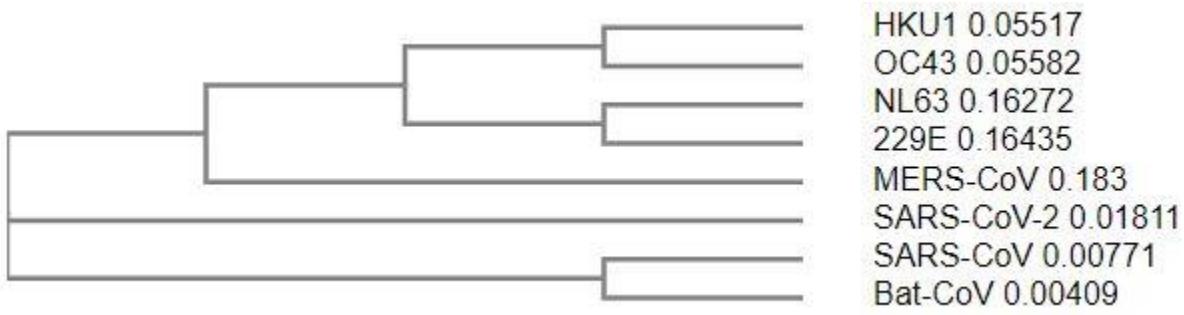


**Figure S1 (b). Phylogenetic Tree showing of HCoVs.**

**Table S1. SARS-CoV-2 RdRp structural information**

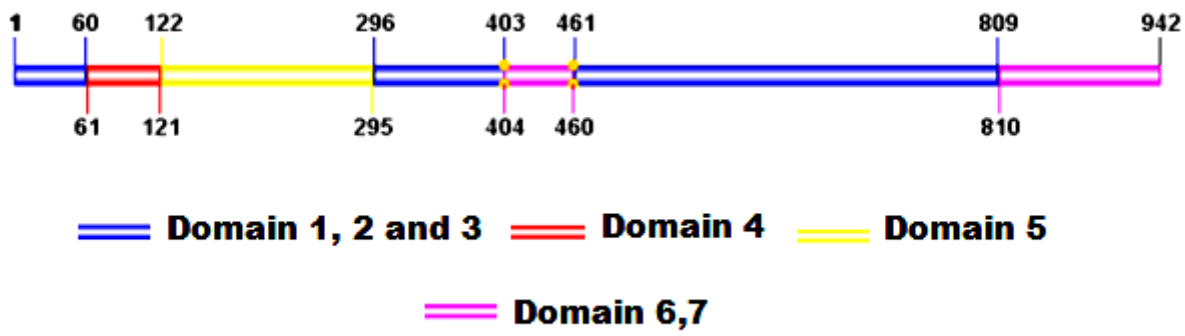


| Protein Chain | AA Range and conformation<br>α-helix (pink); β-sheet (yellow) |
|---|---|
| 6m71_Chain A | 1-942 (1-60, 296-403, 461-809; Domain 1)<br>33---40 β-sheet; 41---45 β-sheet; 46---49 β-sheet; 61-121 (Domain 2); 71---74 β-sheet; 77---90 α-helix; 98---101 β-sheet; 113---118 β-sheet; 122-295 (Domain 3); 124---133 α-helix; 140---149 α-helix; 170---177 α-helix; 179-198 α-helix; 199-205 β-sheet; 209-212 β-sheet; 214-217 β-sheet; 222-228 β-sheet; 230-234 β-sheet; 230---234 β-sheet; 235---242 α-helix; 276---286 α-helix; 304---317 α-helix; 326---336 α-helix; 338---349 β-sheet; 350---356 β-sheet; 361---364 β-sheet; 368---376 α-helix; 378---385 α-helix; 396---400 β-sheet; 404-460, 810-942 Domain 4; 407---416 β-sheet; 418---426 α-helix; 441---446 β-sheet; 448---455 α-helix; 466---480 α-helix; 500-513 motif G; 512---519 α-helix; 521---533 α-helix; 538-560 motif F; 539---545 β-sheet; 555---561 β-sheet; 563---581 α-helix; 597---606 α-helix; 611-627 motif A; 611---617 β-sheet; 648---661 α-helix; 663---670 β-sheet; 671---678 β-sheet; 680-709 motif B; 687---709 α-helix; 718---732 α-helix; 739---751 α-helix; 752---759 β-sheet; 760---766 β-sheet; 767---774 α-helix; 775-796 motif D; 779---788 α-helix; 779---803 β-sheet; 810---821 motif E; 815---823 β-sheet; 824---832 β-sheet; 834---841 α-helix; 842---845 β-sheet; 853---866 α-helix; 877---893 α-helix<br><br>SADAQSFLNRVCGVSAARLTPCGTGTSTDVVYRAFDIYNDKVAGFAKFLKTNCC<br>RFQEKDEDDNLIDSYF<br>VVKRHTFSNYQHEETIYNLLKDCPAVAKHDFFKFRIDGDMVPHISRQRLTKYTM<br>ADLVYALRHFDEGNCD<br>TLKEILVTYNCCDDDYFNKKDWYDFVENPDILRVYANLGERVRQALLKTVQFC<br>DAMRNAGIVGVLTLDNQ<br>DLNGNWYDFGDFIQTTPGSGVPVVDSYYSLLMPILTLTRALTAESHVDTDLTKPY<br>IKWDLLKYDFTEERL<br>KLFDRYFKYWDQTYHPNCVNCLDDRCILHCANFNVLFSTVFPPTSFGPLVRKIFV<br>DGVPFVVSTGYHFRE<br>LGVVHNQDVNLHSSRLSFKELLVYAADPAMHAASGNLLLDKRTTCFSVAALTN<br>NVAFQTVKPGNFNKDFY<br>DFAVSKGFFKEGSSVELKHFFFAQDGNAAISDYDYYRYNLPTMCDIRQLLFVVE<br>VVDKYFDCYDGGCINA<br>NQVIVNNLDKSAGFPFNKWGKARLYYDSMSYEDQDALFAYTKRNVIPTITQMN |

| | |
|---|---|
| | LKYAISAKNRARTVAGV<br>SICSTMTNRQFHQKLLKSIAATRGATVVIGTSKFYGGWHNMLKTVYSDVENPHL<br>MGWDYPKCDRAMPNML<br>RIMASLVLARKHTTCCSLSHRFYRLANECAQVLSEMVMCGGSLYVKPGGTSSGD<br>ATTAYANSVFNICQAV<br>TANVNALLSTDGNKIADKYVRNLQHRLYECLYRNRDVDTDFVNEFYAYLRKHF<br>SMMILSDDAVVCFNSTY<br>ASQGLVASIKNFKSVLYYQNNVFMSEAKCWTETDLTKGPHEFCSQHTMLVKQG<br>DDYVYLPYPDPSRILGA<br>GCFVDDIVKTDGTLMIERFVSLAIDAYPLTKHPNQEYADVFHLYLQYIRKLHDEL<br>TGHMLDMYSVMLTND<br>NTSRYWEPEFYEAMYTPHTVLQHHHHHHHHHH |
| 6m71_Chain B | 1-198 (118-198 Domain 6)<br>81---97 α-helix; 101---108 α-helix; 126---133 β-sheet; 135---142 α-helix; 146---150 β-sheet; 151---155 β-sheet; 156---162 β-sheet; 183---190 β-sheet<br><br>AIASEFSSLPSYAAFATAQEAYEQAVANGDSEVVLKKLKKSLNVAKSEFDRDAA<br>MQRKLEKMADQAMTQM<br>YKQARSEDKRAKVTSAMQTMLFTMLRKLDNDALNNIINNARDGCVPLNIIPLTT<br>AAKLMVVIPDYNTYKN<br>TCDGTTFTYASALWEIQQVVDADSKIVQLSEISMDNSPNLAWPLIVTALRANSAV<br>KLQ |
| 6m71_Chain C | 1-83<br>4---20 α-helix; 26---41 α-helix; 46---59 α-helix<br><br>SKMSDVKCTSVVLLSVLQQLRVESSSKLWAQCVQLHNDILLAKDTTEAFEKMVS<br>LLSVLLSMQGAVDINK<br>LCEEMLDNRATLQ |
| 6m71_Chain D | 1-198<br>87---98 α-helix; 101---110 α-helix; 114---117 β-sheet; 129---132 β-sheet<br><br>AIASEFSSLPSYAAFATAQEAYEQAVANGDSEVVLKKLKKSLNVAKSEFDRDAA<br>MQRKLEKMADQAMTQM<br>YKQARSEDKRAKVTSAMQTMLFTMLRKLDNDALNNIINNARDGCVPLNIIPLTT<br>AAKLMVVIPDYNTYKN<br>TCDGTTFTYASALWEIQQVVDADSKIVQLSEISMDNSPNLAWPLIVTALRANSAV<br>KLQ |

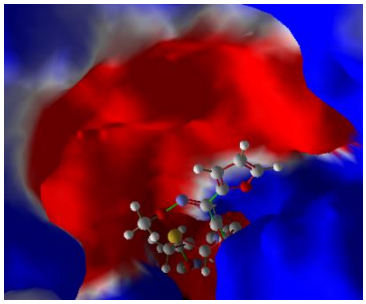

**Cefuroxime**

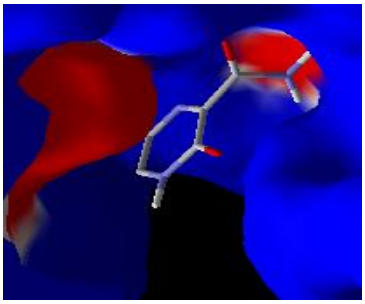

**Avigan**

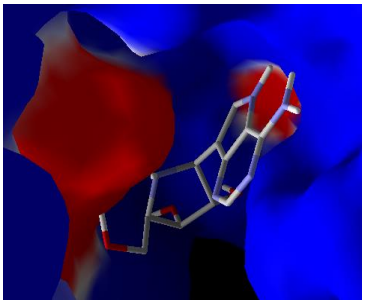

**Galidesivir**

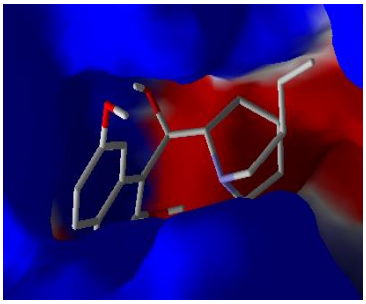

**HCQ**

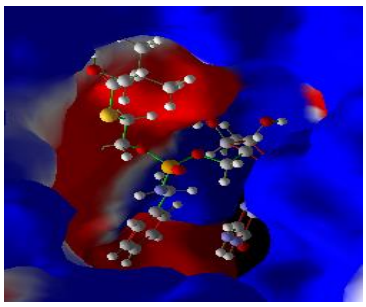

**IDX-184**

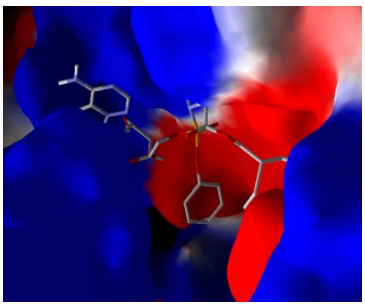

**Remdesivir**

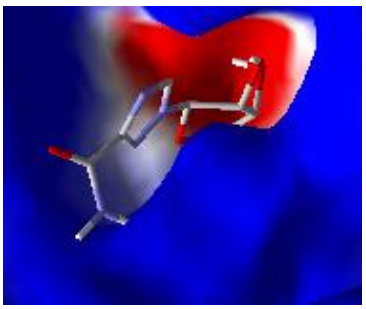

**Ribavirin**

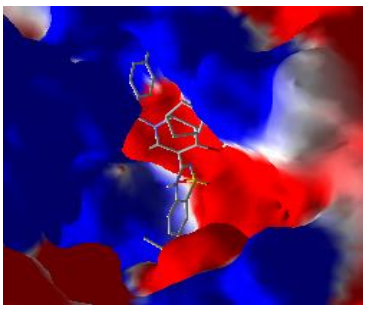

**Setrobuvir**

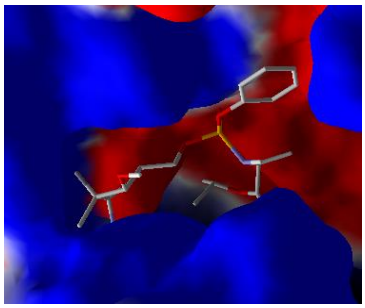

**Sofosbuvir**

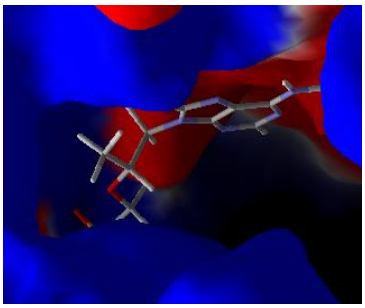

**Tenofovir**

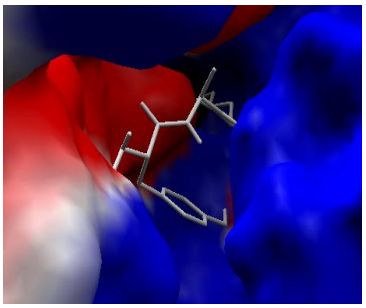

**YAK**

**FigureS2. Catalytic site binding of known drugs with SARS-CoV-2 RdRp**

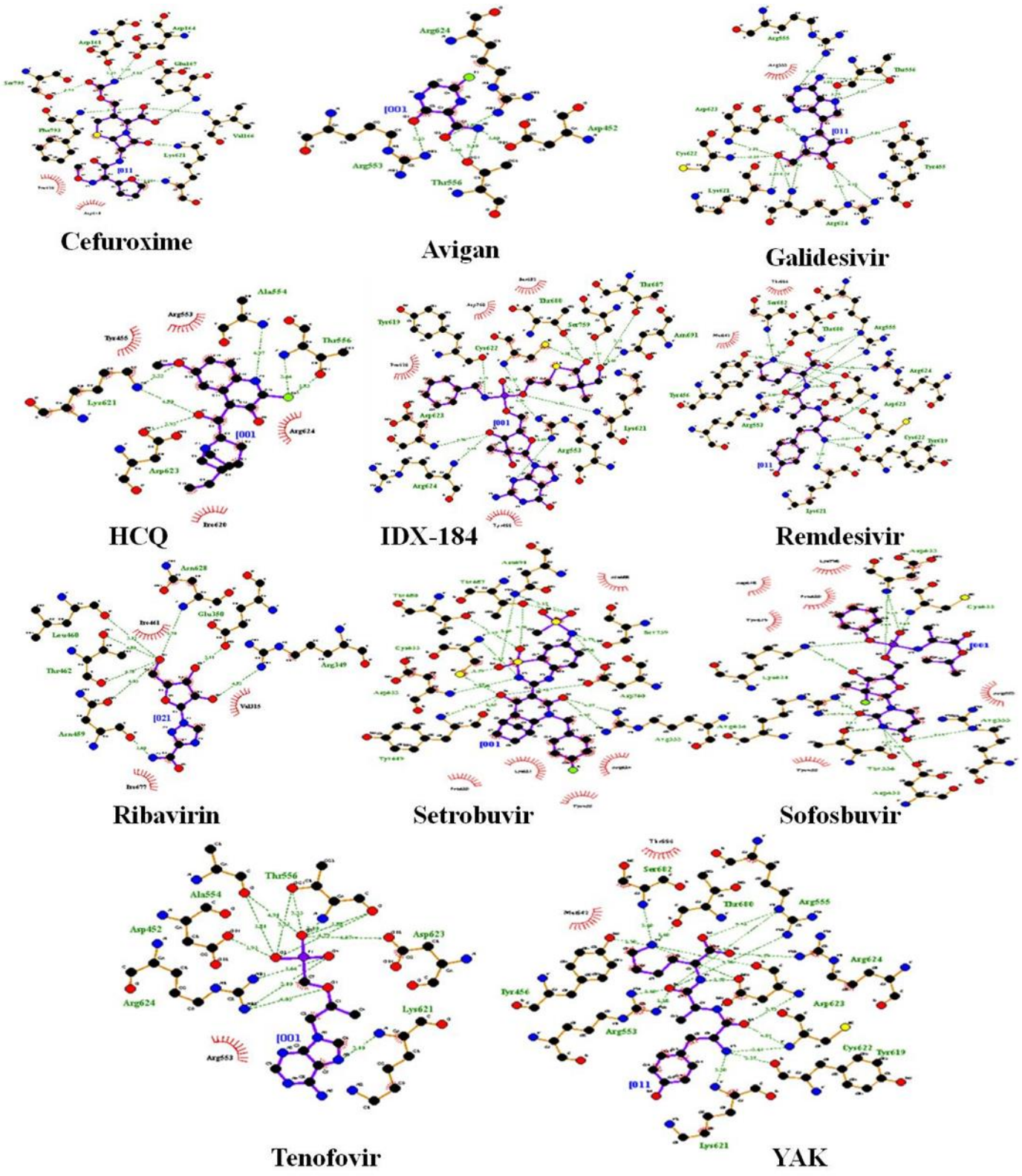


**FigureS3. Interaction of known/commercial drugs with the AA residues in the binding pocket of SARS-CoV-2 RdRp.**